

## The effects of exchange bias on Fe–Co/MgO magnetic nanoparticles with core/shell morphology

This article has been downloaded from IOPscience. Please scroll down to see the full text article.

2010 J. Phys.: Condens. Matter 22 026004

(<http://iopscience.iop.org/0953-8984/22/2/026004>)

View [the table of contents for this issue](#), or go to the [journal homepage](#) for more

Download details:

IP Address: 129.252.86.83

The article was downloaded on 30/05/2010 at 06:32

Please note that [terms and conditions apply](#).

# The effects of exchange bias on Fe–Co/MgO magnetic nanoparticles with core/shell morphology

C Martínez-Boubeta<sup>1,3</sup>, LI Balcells<sup>1</sup>, C Monty<sup>2</sup> and B Martínez<sup>1,4</sup>

<sup>1</sup> Instituto de Ciencia de Materiales de Barcelona (ICMAB-CSIC), Campus UAB, 08193 Bellaterra, Spain

<sup>2</sup> CNRS/Procédés, Matériaux et Energie Solaire (PROMES), 66120 Font Romeu, France

E-mail: [ben.martinez@icmab.es](mailto:ben.martinez@icmab.es)

Received 2 October 2009, in final form 12 November 2009

Published 9 December 2009

Online at [stacks.iop.org/JPhysCM/22/026004](http://stacks.iop.org/JPhysCM/22/026004)

## Abstract

The effects of exchange bias on core/shell structured nanoparticles are analyzed. Nanoparticles are integrated with high moment Fe–Co crystallites covered epitaxially with MgO shells. It is observed that the coercive field  $H_C(\text{FeCo}) > H_C(\text{Co}) > H_C(\text{Fe})$ ; however, the exchange bias field  $H_E$  of the Co sample is higher than that of the FeCo one, while  $H_E = 0$  for the Fe sample. It is suggested that the exchange bias is induced by the formation of a (Co, Mg)O solid solution. In fact, we show that it is possible to modify the exchange bias properties by manipulating the level of Mg dusting at the interface, as recently reported for thin films.

(Some figures in this article are in colour only in the electronic version)

Magnetic materials with reduced dimensionalities have been actively pursued for a broad range of applications. For instance, granular metal/insulator composites, in which nanoparticles of a high moment magnetic metal are embedded in a nonmagnetic insulating matrix (such as  $\text{AlO}_x$ ,  $\text{Hf}_2\text{O}_3$ ,  $\text{Cr}_2\text{O}_3$ , or  $\text{SiO}_x$ ), might pave the way toward gigahertz data rates in magnetic recording [1]. But magnetic nanoparticles are also worth investigating to obtain a deepened understanding of fundamental magnetic properties. A reduction of the net magnetic moment as compared to that of the bulk counterpart is typically observed in magnetic nanoparticles. This is due to a certain degree of disorder at the surface due to broken symmetry, roughness, variation of the chemical stoichiometry, etc. In appropriate circumstances this disorder might give rise to interesting proximity effects such as exchange bias (EB), that manifests itself through shifted hysteresis loops caused by an EB field,  $H_E$  [2–5]. EB arises from direct exchange interactions at the interface between ferromagnetic and antiferromagnetic (AF) systems and may be useful for stabilizing magnetic moments of small ferromagnetic

particles [6], thus becoming a subject of increasing research interest.

In comparison to layered systems, nanocrystals benefit from curvature inducing spin disorder that might increase the uncompensated spin densities produced by finite size considerations. Recent studies have shown that  $H_E$  can be further increased by augmenting the density of uncompensated interfacial AF spins by dilution with a nonmagnetic atom [7, 8]. In these studies the formation of a solid solution between CoO and MgO was held responsible for the boosting of exchange bias effects [9, 10].

FeCo alloys are of interest because they have superior magnetic properties, but they suffer from easy oxidation. Thus active research has been maintained looking for the most appropriate capping to protect magnetic nanoparticles against oxidation with little disruption of their magnetic properties [11]. It is at this point that MgO capping offers interesting possibilities, as demonstrated for Co/MgO bilayer films [7]. Thus, in this work we analyze the exchange bias phenomenon for Fe–Co alloy crystalline nanoparticles capped with MgO. We have studied several samples containing progressive additions of Co, from pure Fe to pure Co, to modify the magnetic properties of the particles while retaining a similar size. Our experiments suggest the formation of

<sup>3</sup> Moving to: IN<sup>2</sup>UB, Departament d'Electrònica, Universitat de Barcelona, 08028, Spain.

<sup>4</sup> Author to whom any correspondence should be addressed.

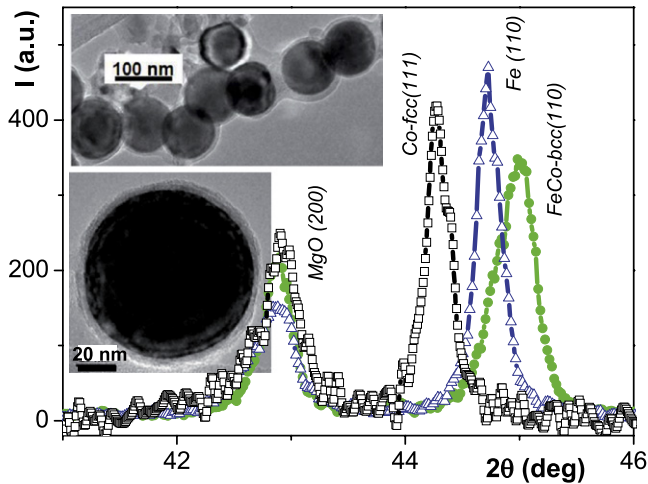


**Figure 1.** Selected MgO(200) diffraction and bcc Fe (blue triangles), Fe–Co alloy (green dots) and fcc Co (black squares) x-ray peaks. Inset: electron microscopy images of the particles with a core/shell structure.

$\text{Mg}_{1-x}\text{Co}_x\text{Fe}_y\text{O}$  at the interface, which causes local exchange anisotropy and EB effects.

Nanoparticles of about 100 nm diameter (see figure 1) were prepared in a single-step process by the vapor-condensation method. The target was prepared by using Fe (purity >99.5%, BASF), Co (Aldrich, 99.8%), and MgO (Alfa Aesar, 99.998%) powders mixed in the desired proportions. Due to the reactivity of 3d metals as regards oxidation, a minute excess of Mg (Aldrich, 99.9%) was used in some cases to provide reducing conditions. The metallic/oxide core/shell structure could be clearly identified by electron microscopy, which shows a core/shell cube-on-cube orientation relationship similar to that usually found in thin films (not shown here) [12–14].

The crystallographic structure of the as-formed particles was further studied by x-ray powder diffraction (XRD) analysis. X-ray patterns for selected samples are shown in figure 1. In the case of Fe/MgO nanoparticles the diffraction peaks corresponding to MgO and  $\alpha$ -Fe were clearly visible. No signals of the presence of  $\text{FeO}_x$  were found. For Co/MgO nanoparticles the formation of the face-centered-cubic (fcc) cobalt phase was detected and no evidence of the formation of either the thermodynamically favored hexagonal-closed-packed (hcp) Co phase or the crystalline oxidic species were found. In FeCo alloyed samples, the bcc FeCo (110) alloy phase peak was found. These results imply that Fe and Co oxides should make only a minor contribution to sample volume fraction, making them difficult to detect with conventional techniques. It is also worth mentioning that the  $c$  lattice parameter for all samples was close to bulk counterpart values within 1% error. For FeCo alloy nanoparticles it was  $c \approx 2.847$  Å, allowing the identification of a bcc crystalline structure, consistent with the bulk Fe–Co phase diagram close to 50% of Fe content [15].

Magnetic measurements (see figure 2) performed using a commercial SQUID magnetometer revealed that at room

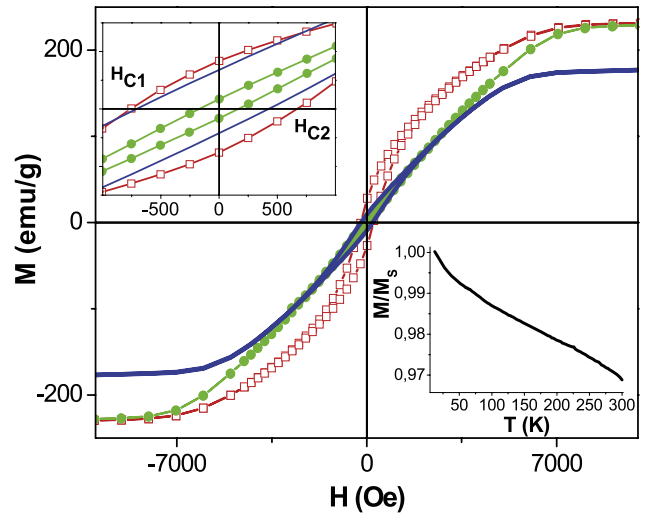


**Figure 2.** Field dependent magnetization curve at room temperature of core/shell nanoparticles with nuclei made of bcc Fe (green spots), Fe–Co alloy (red squares) and fcc Co (blue line). Inset: (upper) detail of the low field region at  $T = 10$  K after cooling samples in 20 kOe; (lower) temperature dependence of the saturation magnetization under an applied field of 20 kOe.

temperature (RT) the saturation magnetization ( $M_S$ ) of our samples, determined by extrapolating the high field linear part to zero field, range between  $\sim 170 \pm 8$  emu  $\text{g}^{-1}$  for the Co sample and  $\sim 220 \pm 5$  emu  $\text{g}^{-1}$  for the FeCo one, close to those of the bulk counterparts [16]. It is clearly observed that increasing the Co content increases the magnetic hardness of the particles, i.e. the coercive field ( $H_C$ ), as depicted in figure 3. It should be mentioned that special care was taken in measuring hysteresis loops in order to avoid effects derived from the remanent field of the superconducting magnet on the determination of  $H_C$ . For that purpose a procedure for reducing the remanent field of the magnet, by charging fields of opposite sign and reduced magnitude down to zero field, was followed before measuring each hysteresis loop. Values close to that estimated for magnetization reversal of spherical single-domain grains [17], with  $H_C(\text{FeCo}) \approx 240$  Oe  $>$   $H_C(\text{Co}) \approx 220$  Oe  $>$   $H_C(\text{Fe}) \approx 130$  Oe, were found.

Considering a system of nanoparticles whose anisotropy is made up of mixed cubic magnetocrystalline and uniaxial components, for a certain range of magnetic fields, the effective anisotropy constant ( $K_{\text{eff}}$ ) can be evaluated from the slope of the initial magnetic susceptibility:  $\chi = \partial M / \partial H \propto K_{\text{eff}}^2 / M_S H^3$ . Thus, an estimate of  $K_{\text{eff}}$  can be obtained from  $\chi$  versus  $1/H^3$  plots (not shown), obtaining values of  $K_{\text{eff}} \approx 4.5 \pm 1.1 \times 10^4$  J  $\text{m}^{-3}$  for bcc Fe at room temperature. The anisotropy for the FeCo/MgO nanoparticles ( $K_{\text{eff}} \approx 5.4 \times 10^4$  J  $\text{m}^{-3}$ ) probably approaches Fe–Co alloy bulk values [18]. For the Co sample with fcc structure, which is only known as a high temperature structural modification, the anisotropy obtained was  $K_{\text{eff}} \approx 3.8 \pm 1 \times 10^4$  J  $\text{m}^{-3}$ , in agreement with the values estimated for fcc Co/Cu (001) multilayers [19].

$M(H)$  magnetization curves at  $T = 10$  K were not fully saturated even at 50 kOe, exhibiting a substantial high field susceptibility (inset in figure 2). This high field susceptibility

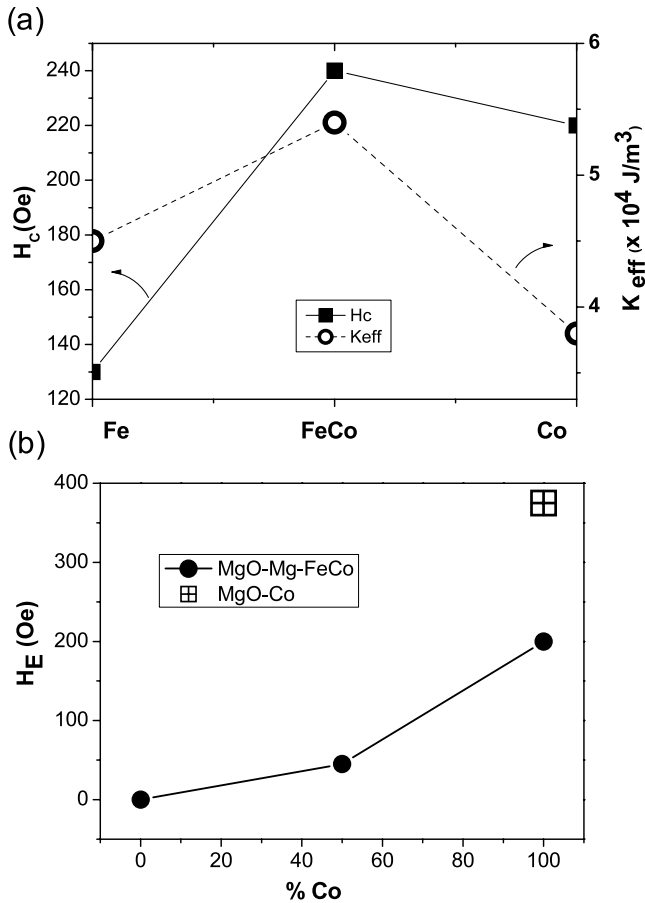


**Figure 3.** (a) Coercive field ( $H_C$ ) and effective anisotropy constant ( $K_{eff}$ ) dependence on composition at room temperature. (b) Exchange bias field ( $H_E$ ) for the three MgO–Mg–Fe–Co samples (dots) at  $T = 10$  K and for the MgO–Co case (square). Experimental errors are about the size of the symbols for the experimental points. Symbols correspond to measured data and lines are guides to the eye.

turned out to be temperature dependent, decreasing drastically as temperature increases. It is worthy of note that  $M_S(T)$  curves measured after cooling the samples in a 20 kOe field also exhibit an abnormal increase of  $M_S$ . These features strongly suggest the existence of uncompensated spins at the interfaces of the particles [20]. Such behavior is normally attributed to the magnetic exchange interactions between neighboring  $(3d)^{2+}$  ions [21].

The effect of surface spin magnetization, might explain the magnetization pinning results shown in figure 2. The presence of small amounts of CoO (which become AF at 290 K) and MgCo<sub>2</sub> (AF below 45 K), undetectable using XRD, would contribute to increased surface pinning, affecting the magnetic behavior. Thus, to study the possible existence of exchange bias phenomena, samples were cooled in a 20 kOe field from RT down to 10 K and the  $M(H)$  curves were measured. The exchange bias field  $H_E = (H_{C1} + H_{C2})/2$ , where  $H_{C1}$  and  $H_{C2}$  are the corresponding values of  $H_C$  for the negative and positive magnetic fields regions, was negative and decreased with increasing temperature, being zero at RT. It was found that  $H_E(\text{Co}) > H_E(\text{FeCo})$  and no EB effects

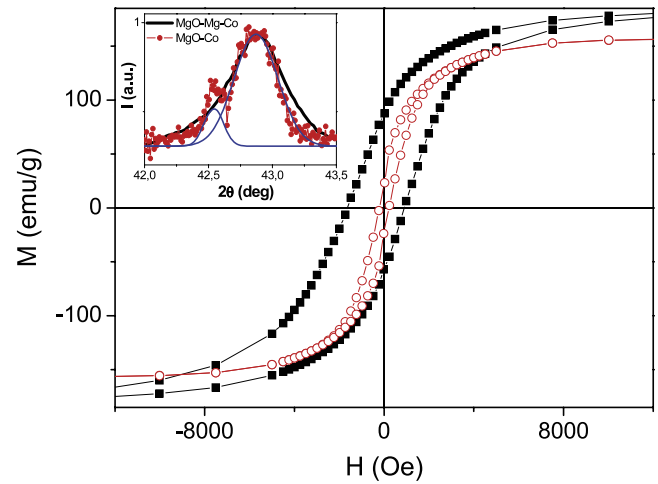


**Figure 4.** High field hysteresis loops for nanocrystals produced from a targeted mixture of MgO and Co, at RT (circles) and 10 K (squares) after a field-cooled experiment at 20 kOe. Inset: (on the left) detail of the MgO(200) diffraction peaks for Co-doped samples containing Mg (heavy line) in comparison with samples where MgO was used alone (dots). The asymmetric peak can be roughly resolved into symmetric peaks at 42.9° (MgO) and 42.5° (Co–MgO solution).

were observed for the Fe sample (figure 3). The observed Fe–Co composition dependence of the exchange bias can be explained on the basis of the well-known dependences  $H_E \propto 1/M_S$  on the magnetization of the FM layer [22]. Also, the observed trend of increasing exchange coupling across the series is most probably associated with the increasing number of 3d electrons, responsible for magnetic superexchange interactions [23].

In fact, the intensity of  $H_E$  will depend on the strength of the AF interactions and the degree of disorder [7], which will vary, as some Co atoms are substituted for Fe or Mg atoms. The significant role of the disorder in increasing  $H_E$  through the dilution with nonmagnetic Mg atoms is further evidenced in figure 4. We show that biasing is enhanced with a dusting of certain magnetic impurities, present at the interface. Whenever MgO was used alone (i.e. no Mg was available to provide reducing conditions and therefore the amounts of atomic oxygen available during the growth are very different in the two cases), an interfacial Mg(Co, Fe)<sub>2</sub>O<sub>4</sub>-like oxide layer was unambiguously detected by means of x-ray magnetic circular dichroism (not shown here) [13]. Stronger bonding with oxygen is expected for Co as compared to Fe at the MgO interface from bond energy considerations, and we speculate that this difference is responsible for the  $H_E$  in the FeCo samples. In the case of FeCo samples, a FeCo–(Co, Mg)O–MgO gradient interface is proposed from models of internal displacement reactions in oxide solid solutions [24]. The inset in figure 4 shows a feature in the XRD at 42.54°, and its intensity decreases dramatically upon Mg addition, revealing unambiguously a more abrupt interface. The corresponding lattice parameter ( $\sim 4.25$  Å) is attributed to the presence of Mg<sub>1-x</sub>Co<sub>x</sub>O solid solution with a cobalt composition close to 0.75 [25]. We surmise that the formation of (Mg, Co)O is driven by the slightly positive enthalpies of mixing. Thus, the



variation in  $H_E$  appears to be the direct result of a change in native oxide stoichiometry, as discussed by Miltényi *et al* [7]. Note that the coercivity at room temperature for the Co/MgO particles is the same as that for the Co/Mg/MgO case (figure 3). Nonetheless, we found the exchange bias shift to be above 350 Oe.

In the mixed (Mg, Co)O, the spacing between  $\text{Co}^{2+}$  ions may differ appreciably from that in CoO. Since the exchange interaction is a rapidly varying function of the atomic separation, we anticipate that the dilution of Mg into CoO must have a significant effect on the exchange bias. Considering the above results for the (Co, Mg)O formation, it is reasonable to assume that the nearest neighbor interactions are increased by the minor addition of Mg to the antiferromagnetic CoO since it decreases the lattice constant (in view of the fact that the ionic radius of  $\text{Mg}^{2+}$  is lower than that of cobalt). Indeed, electronic structure calculations have shown that the closer the atoms are, the larger the overlap between the Co d orbitals and the oxygen p orbitals is, therefore increasing the Heisenberg exchange parameters [23]. Thus, our interpretation might be considered complementary to the domain state model for defect-induced EB enhancement used by Miltényi *et al* [7] to explain the strong increase of exchange bias with the Mg dilution before it drops for concentrations above 0.3.

It is noteworthy that in the past few years various theoretical studies have discussed the effects of impurities in a low dimensional antiferromagnet [26, 27]. Results based on quantum Monte Carlo simulations suggest that one would indeed expect to find an enhancement of the antiferromagnetic order for the case of a nonmagnetic impurity. For sufficiently large impurity concentrations, the reduced connectivity between  $\text{Co}^{2+}$  ions next to the impurity site would decrease the antiferromagnetic order. At a more speculative level, we note that in stoichiometric CoO,  $\text{Co}^{2+}$  is high spin, and dilution with Mg probably retains the characteristic features of high spin  $\text{Co}^{2+}$ . However, as for Li-doped NiO [28], we are probably decreasing the number of states in the antibonding O 2p–Co 3d hybridized orbitals by decreasing the lattice parameter for CoO compared to (Co, Mg)O. On the other hand, first-principles calculations showed that the shorter Fe–O bond length in magnesiowüstite compared to FeO leads the octahedral symmetry to break a gap within the minority  $t_{2g}$  states [29]. It is plausible that it exists in CoO as well. Thus, when a sufficiently high Mg doping level is reached, it may become advantageous to drain the  $e_g$  orbitals, so the Co may eventually reach a low spin ground state (for instance,  $t_{2g}^6 e_g^1$ ). This would cause a lessening of the exchange bias effects.

In summary, we reported here the behavior of core–shell particles in which both the core and shell microstructures are very well defined, and the size distribution is narrow. We have explored variations in the composition of the ferromagnetic core from pure Co to pure Fe. Our results resemble those provided by Rohart *et al* [30] for chemically disordered fcc CoPt clusters in a MgO matrix, with an enhanced surface anisotropy due to the partial oxidation at the interface. Thus, the enhanced exchange bias effect is likely to be due to a change in the oxide stoichiometry at the interface. It is proposed that all the examples of locally enhanced

antiferromagnetism near a vacancy which have been studied independently in the literature may have a simple common explanation. For instance, unlike the case reported by Miltényi *et al* [7], where a domain state model for defects inducing EB enhancement is used, we assume that the closer the atoms are, the larger the overlap between the Co d orbitals and the oxygen p orbitals is, therefore increasing the  $H_E$ . For large dilution,  $H_E$  again decreases as the antiferromagnetic order is increasingly suppressed by the diminishing electron correlation between  $\text{Co}^{2+}$  ions.

## Acknowledgments

We acknowledge financial support from Spanish MICINN (MAT2009-08024 and Consolider-Ingenio CSD2007-00041) projects. This work was also partially funded by the EU under the ‘SOLFACE’ project in the framework of the 6<sup>e</sup> PCRDT program and by the FEDER program. C M Boubeta acknowledges financial support through the Ramón y Cajal program.

## References

- [1] Beach G S D and Berkowitz A E 2005 *IEEE Trans. Magn.* **41** 2043
- [2] Nogués J and Schuller I K 1999 *J. Magn. Magn. Mater.* **192** 203
- [3] Iglesias O, Batlle X and Labarta A 2008 *J. Phys. D: Appl. Phys.* **41** 134010
- [4] Inderhees S E, Borchers J A, Green K S, Kim M S, Sun K, Strycker G L and Aronson M C 2008 *Phys. Rev. Lett.* **101** 117202
- [5] Khac Ong Q, Wei A and Lin X M 2009 *Phys. Rev. B* **80** 134418
- [6] Skumryev V, Stoyanov S, Zhang Y, Hadjipanayis G, Givord D and Nogués J 2003 *Nature* **423** 850
- [7] Miltényi P, Gierlings M, Keller J, Beschoten B, Güntherodt G, Nowak U and Usadel K D 2000 *Phys. Rev. Lett.* **84** 4224
- [8] Hong J-I, Leo T, Smith D J and Berkowitz A E 2006 *Phys. Rev. Lett.* **96** 117204
- [9] Ghadimi M R, Beschoten B and Güntherodt G 2005 *Appl. Phys. Lett.* **87** 261903
- [10] Leo T, Hong J-I, Smith D J and Berkowitz A E 2007 *J. Appl. Phys.* **102** 123904
- [11] Arbiol J, Peiró F, Cornet A, Clavero C, Cebollada A, Armelles G and Huttel Y 2005 *Appl. Phys. Lett.* **86** 032510
- [12] Martinez-Boubeta C, Balcells L, Monty C, Ordejón P and Martínez B 2009 *Appl. Phys. Lett.* **94** 062507
- [13] Martinez-Boubeta C, Balcells L, Monty C and Martínez B 2009 *Appl. Phys. Lett.* **94** 262507
- [14] Martinez-Boubeta C *et al* 2009 *Nanomed.: Nano. Bio. Med.* at press (doi:10.1016/j.nano.2009.09.003)
- [15] Hansen M 1958 *Constitution of Binary Alloys* (New York: McGraw-Hill)
- [16] Kuhrt Ch and Schultz L 1992 *J. Appl. Phys.* **71** 1896
- [17] Tamura I J 1995 *J. Magn. Magn. Mater.* **145** 327
- [18] Morrish A H 1965 *The Physical Principles of Magnetism* (New York: Wiley)
- [19] Hillebrands B, Fassbender J, Jüngleblut R, Gunderot G, Roberts D and Gehring G 1996 *Phys. Rev. B* **53** R10548
- [20] Murayama A, Hiller U, Hyomi K, Oka Y and Falco C M 2002 *J. Magn. Magn. Mater.* **240** 355
- [21] Mielejohn W H and Bean C P 1957 *Phys. Rev.* **105** 904
- [22] Kirkpatrick E M, Leslie-Pelecky D L, Kim S-H and Rieke R D 1999 *J. Appl. Phys.* **85** 5375
- [23] Wu X W and Chien C L 1998 *Phys. Rev. Lett.* **81** 2795

- [23] Fischer G, Däne M, Ernst A, Bruno P, Lüders M, Szotek Z, Temmerman W and Hergert W 2009 *Phys. Rev. B* **80** 014408
- [24] Reddy S N S, Leonard D N, Wiggins L B and Jacob K T 2005 *Metall. Mater. Trans. A* **36** 2695
- [25] Wang L, Navrotsky A, Stevens R, Woodfield B F and Boerio-Goates J 2003 *J. Chem. Thermodyn.* **35** 1151
- [26] Martins G B, Laukamp M, Riera J and Dagotto E 1997 *Phys. Rev. Lett.* **78** 3563
- [27] Engel J and Wessel S 2009 *Phys. Rev. B* **80** 094404
- [28] de Groot F M F, Abate M, van Elp J, Sawatzky G A, Ma Y J, Chen C T and Sette F 1993 *J. Phys.: Condens. Matter* **5** 2277
- [29] Tsuchiya T, Wentzcovitch R M, da Silva C R S, de Gironcoli S and Tsuchiya J 2006 *Phys. Status Solidi b* **243** 2111
- [30] Rohart S, Raufast C, Favre L, Bernstein E, Bonet E and Dupuis V 2006 *Phys. Rev. B* **74** 104408